
A SCALABLE FRAMEWORK FOR ACCELERATION OF CNN TRAINING ON DEEPLY-PIPELINED FPGA CLUSTERS WITH WEIGHT AND WORKLOAD BALANCING

A PREPRINT

Tong Geng
Boston University
tgeng@bu.edu

Tianqi Wang
Boston University
tianqi@bu.edu

Ang Li
Pacific Northwest National Laboratory
ang.li@pnnl.gov

Xi Jin
University of Science and Technology of China
jinxi@ustc.edu.cn

Martin Herbordt
Boston University
herbordt@bu.edu

February 28, 2022

ABSTRACT

Deep Neural Networks (DNNs) have revolutionized numerous applications, but the demand for ever more performance remains unabated. Scaling DNN computations to larger clusters is generally done by distributing tasks in batch mode using methods such as distributed synchronous SGD. Among the issues with this approach is that to make the distributed cluster work with high utilization, the workload distributed to each node must be large, which implies nontrivial growth in the SGD mini-batch size.

In this paper, we propose a framework called FPDeep, which uses a hybrid of model and layer parallelism to configure distributed reconfigurable clusters to train DNNs. This approach has numerous benefits. First, the design does not suffer from batch size growth. Second, novel workload and weight partitioning leads to balanced loads of both among nodes. And third, the entire system is a fine-grained pipeline. This leads to high parallelism and utilization and also minimizes the time features need to be cached while waiting for back-propagation. As a result, storage demand is reduced to the point where only on-chip memory is used for the convolution layers. We evaluate FPDeep with the Alexnet, VGG-16, and VGG-19 benchmarks. Experimental results show that FPDeep has good scalability to a large number of FPGAs, with the limiting factor being the FPGA-to-FPGA bandwidth. With 6 transceivers per FPGA, FPDeep shows linearity up to 83 FPGAs. Energy efficiency is evaluated with respect to GOPs/J. FPDeep provides, on average, 6.36x higher energy efficiency than comparable GPU servers.

Keywords Convolution Neural Network Training · Reconfigurable Computing · Parallel and Distributed Systems

1 Introduction

Deep convolutional neural networks (CNNs) have revolutionized applications such as image classification and object recognition [1, 2, 3, 4]. As there remains an open-ended demand for more complex networks and larger datasets, new computing solutions are critical.

Distributed synchronous stochastic gradient descent (SGD) has enabled large-scale CNN training by partitioning SGD mini-batches into smaller data batches that can then be processed in parallel and so accelerate CNN training [5]. A drawback of this method is scalability: to enable continued high utilization as the number of nodes increases, each node must be allocated an ever larger workload. But larger mini-batches slow training convergence. Thus, while larger clusters provide increased computation capacity, the training time is not proportionally reduced [5].

FPGA clusters are recognized to be a competitive technology for CNN inference [6, 7, 8, 9, 10, 11, 12, 13]. For CNN training, however, their efficacy is still an open question; one that is addressed in this work. Previous FPGA clusters for CNN training have generally worked in batch mode (*batch* in the computational sense), which uses the distributed synchronous SGD algorithm just described [14, 15, 16, 17, 18, 19]. In this approach, called *Data-Parallelism* [20], each FPGA executes all layers of the CNN. This is done in sequential order, a layer at a time, and a new layer starts only after the previous one has completed. Data-Parallelism has three significant disadvantages. First, optimal FPGA configurations for the different CNN layers vary greatly. Therefore, either the FPGA is suboptimally configured, or the FPGA needs to be reconfigured repeatedly at run-time. Second, storage required for weights and intermediate features is generally large enough that off-chip memory must be used. And third, this entire approach suffers from the scalability problem of the distributed synchronous SGD algorithm.

Another method, which we call *Layer Parallelism*, is to daisy-chain multiple FPGAs and map the entire CNN onto a single pipeline. Zhang et al. [6] have used Layer Parallelism to accelerate CNNs using FPGA clusters, though only for inference. Their approach, however, still leaves two problems. First, the pipeline is not seamless; a particular layer might be stalled until the previous layer is finished. All features must, therefore, be cached until the last feature of a layer is obtained. This requires large storage that necessitates the use of off-chip memory. Second, the computational intensity varies greatly among layers. A naive workload distribution can therefore result in a large number of idle cycles due to inter-layer dependencies. These two problems exist in both inference and training, but have a greater impact on the latter. In training, all features of the hidden layers must be cached until their corresponding errors arrive through Back Propagation (BP), thus requiring much larger memory. Moreover, due to BP, the number of operations per layer triples.

We propose FPDeep, a novel FPGA-cluster-based training framework for CNNs that solves the problems just described. FPDeep does this by using a hybrid of layer and model parallelism (described below) together with a number of new workload/weight balancing strategies. No reconfiguration is needed: each device computes only certain layers, or a part of a single layer; each device is optimized independently with respect to its own computation. The cluster is now a single fine-grained pipeline so the batch size can be arbitrarily small. The amount of data that must be saved is drastically reduced eliminating most off-chip memory accesses. Internode communication is simple and pipeline utilization very high. To the best of our knowledge, our work is the first framework of CNN training on FPGA-based clusters using this method of parallelism and also the first framework with fine-grained workload/weight balancing.

The underlying theme of this work is to convert batch parallelism to pipeline parallelism, which has obvious benefits. Parallelism is equal to the depth of the pipeline, in this case many thousands of stages across the cluster. Communication paths can be short so cycle times are as small as the designer can make them. Communication among devices is direct and contention-free with any latency having no effect on throughput. There is also the aforementioned benefit of having all of the latency reduction applied to individual problem instances and so obviating the algorithmic challenges that come with larger batches.

We find this approach to be effective with performance similar to that of GPU clusters of similar size and technology, but with far better power efficiency. The limiting factor is inter-FPGA bandwidth. But, somewhat surprisingly, we find that a 1D topology suffices and that, even using only six transceivers per FPGA, FPDeep achieves linear speed-up to 83 FPGAs. The main contributions are as follows:

- The possibility to break down the well-known scalability wall of CNN training and the demonstration of FPGA clusters as a competitive technology for CNN training;
- A novel framework for mapping CNN training logic to distributed FPGA clusters that achieves both high efficiency and scalability; that does not suffer from issues related to mini-batch size; and that needs only a simple interconnection network as is available in any multi-FPGA system with consistent communication and reasonable bandwidth;
- A fine-grained pipeline design that minimizes the time that features need to remain available while waiting for back-propagation, thus reducing the storage demand to the point where only on-chip memory is required for the convolution layers;
- Fine-grained partitioning and mapping methodologies, which provide almost perfect workload and weight balancing among FPGAs; this is done by increasing the flexibility of workload and weight allocation, thus leading to improved utilization: multiple FPGAs can cooperatively compute the same layer, while multiple layers can also be mapped to the same device;
- An RTL code generator that automatically creates RTL implementations based on the mapping scheme generated by FPDeep.

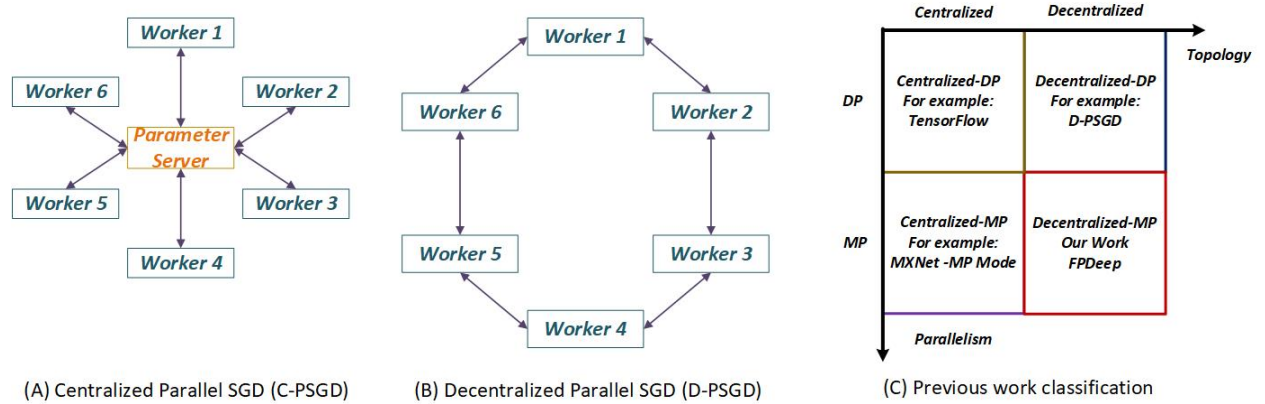


Figure 1: Methods for parallel CNN training

The organization of this paper is as follows. In Section II, related work is discussed. In Section III, the methodology of FPDeep is presented and the workload/weight balanced partition methods are defined. In Section IV, the overall architecture and design of FPDeep accelerators are discussed. In Section V, experimental results are given. Finally, we conclude and suggest further work in Section VI.

2 Design Space and Related Work

Much work has addressed the mapping of inference/training of CNNs to clusters with programmable accelerators, including [21, 4]. Many frameworks and libraries have been deployed, e.g., MXNet [22], Caffe [23], and Tensorflow [24]. These systems hide the complexity of workload decomposition and provide friendly programmer interfaces, including Python, R, and Scala. For FPGA-based clouds, the prior work is more limited. Microsoft’s Catapult project [25, 26] implements a parameterized CNN accelerator cluster which can deliver over 1 TFLOPS with very high energy efficiency. Zhang’s CDSC FPGA-Enabled Cluster accelerates CNNs on top of Spark and Hadoop [16, 6]. In [6], researchers build a deeply pipelined FPGA cluster with 6 Xilinx VC709 boards to accelerate CNNs. In [14], an FPGA-based framework of CNN training is proposed, but focuses mainly on single-FPGA designs.

Most distributed CNN systems, including TensorFlow and CNTK, are based on the distributed synchronous SGD algorithm (Centralized Parallel SGD algorithm - C-PSGD, see Fig.1(A)). The Parameter Server Topology [27] uses a central parameter node connected with multiple worker nodes. Clearly, there are several bottlenecks: communication load on the central node [28] and idle time waiting for straggling worker nodes [29]. Also, for large-scale clusters, the growth in the SGD mini-batch size limits scalability. Lian, et al. use a decentralized parallel SGD algorithm (D-PSGD) to build a large-scale cluster [28]. As shown in Fig.1(B)) each node must maintain its own local copy of the model and data duplication is inevitable. We complete the taxonomy of mapping CNN applications to distributed clusters in the remainder of Fig.1. Fig.1(C) shows the primary design choices: note the present work is decentralized/MP.

Fig.2 shows the design space for mapping CNNs onto distributed nodes. We use terminology introduced by [20].

Data parallelism (Fig.2(A)) is the most popular approach in CPU and GPU clouds [22, 24]. It is also widely used in existing FPGA clouds, such as Catapult and CDSC [16]. This method has drawbacks as mentioned in Section I. In CNNs, the configurations of each layer, such as kernel size, pooling size, and stride size, vary greatly, requiring different hardware designs to obtain optimal performance. Thus, FPGAs need to be reconfigured between layers, leading to significant overhead. In addition, as each FPGA executes all layers in sequential order, each layer starts only after the previous layer has completed. Thus, for all intermediate features, weights need to be stored to and loaded from the host upon completion of a layer, leading to heavy communication with off-chip memory.

Layer Parallelism (Fig.2(B)) maps layers of the CNN onto individual nodes and pipelines CNN computation. It has been employed by both GPU and FPGA frameworks. In [30], multiple GPUs are used in a pipelined manner. Each LSTM layer is assigned to a different GPU. After GPU 1 finishes computing layer 1 for the first sentence, it passes its output to GPU 2. At the same time, GPU 1 fetches the next sentence and starts training. In their work, each layer is allocated with a certain GPU, thus, workloads are not balanced among devices. For multi-FPGA systems, Zhang et al. [6] only focuses on inference; also, the parallelism is coarse-grained, the workload is unbalanced, and there is heavy off-chip memory communication. So while Layer Parallelism mitigates some of the problems with batch size

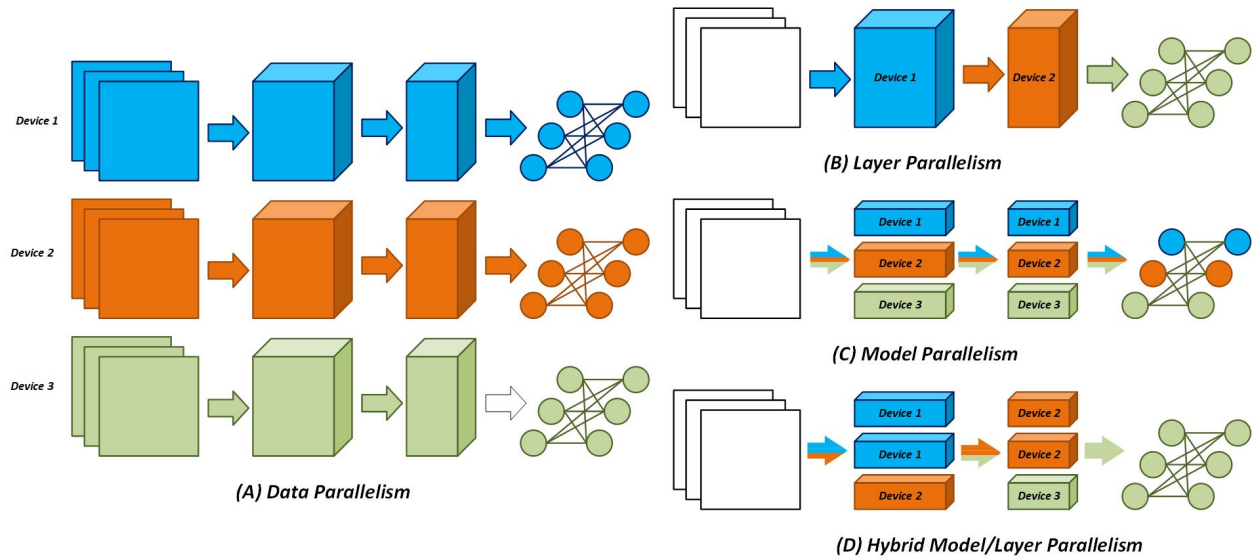


Figure 2: Parallel CNN training: design space of node/layer mappings

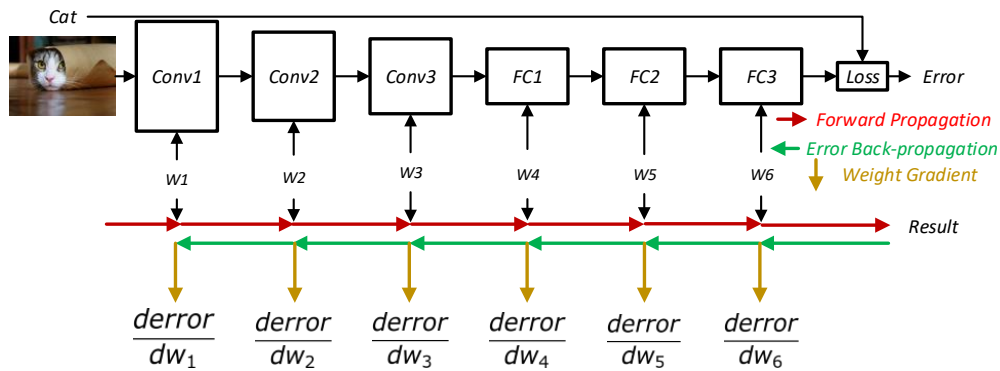


Figure 3: Illustration of computations involved in DNN training

and frequent reconfiguration, it suffers from other problems: load balancing and stalls as some nodes wait for others to finish.

In Model Parallelism (Fig.2(C)), weights for each layer are distributed across nodes. Therefore, all intermediate results from all devices must be added up and then broadcast to every device leading to heavy communication. This method has been used for AlexNet [31].

Hybrid mappings are also possible, e.g., between Model and Layer Parallelism as shown in Fig.2(D) and used in FPDeep. This approach combines the balanced load of Model Parallelism with the simple communication of Level Parallelism. There are several potential problems with Hybrid Parallelism including finding the best partition, the complexity in intra- and inter-layer communication, and handling storage of the weights; we address these in the next sections.

3 FPDeep Methods and Design

3.1 Preliminaries

In this subsection, we review basics of CNN training and define the most important parameters used by FPDeep. A six layer CNN (in Fig.3) is used as an example. The red datapath refers to Forward Propagation (FP). It calculates the errors

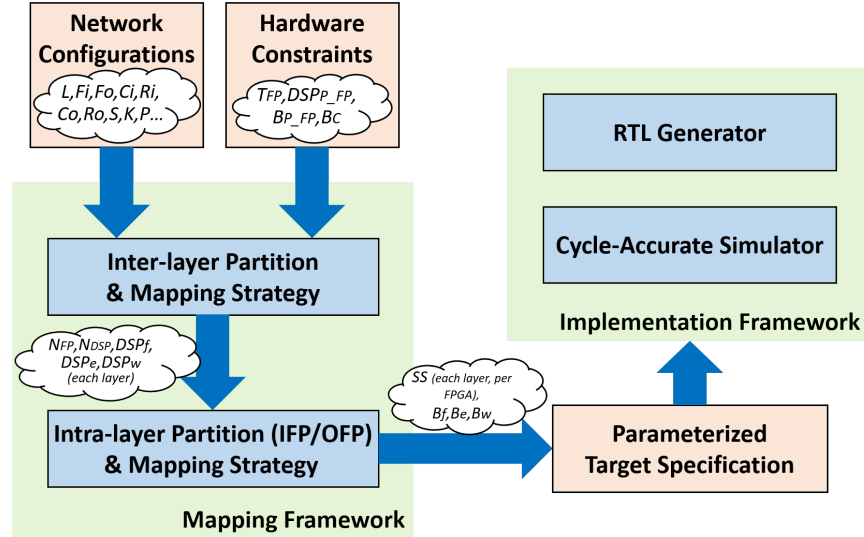


Figure 4: Overview of FPDeep Framework

Table 1: IMPORTANT INPUT AND OUTPUT PARAMETERS USED IN FPDEEP

	Symbol	Description
Network Configuration Parameters	$IC[l]$	Number of layer l input feature map channels
	$OC[l]$	Number of layer l output feature map channels
	$R[l]$	Row num of layer l input feature map
	$C[l]$	Column num of layer l output feature map
	$KW[l]$	Width of layer l convolution kernel
	$KH[l]$	Height of layer l convolution kernel
	$P[l]$	Layer l pooling size
	$PF[l]$	Layer l pooling function
	$AF[l]$	Layer l activation function
Hardware Constraint Parameters	N	Number of FPGA devices in the cluster
	LUT_{max}	Number of Look-up table per FPGA
	FF_{max}	Number of Flip-flop per FPGA
	$BRAM_{max}$	Number of BRAM per FPGA
	DSP_{max}	Number of DSP per FPGA
	$TRANS_{max}$	Number of transceiver per FPGA

of output features in the final layer. Starting with an input image (Cat), neurons in each layer are evaluated with weights w_i . Errors are calculated by comparing inference results to the label ‘‘Cat’’ in the training dataset. BP has two sub-steps: Error Back-propagation (EB-green) and Weight Gradient calculation (WG-orange). In EB, errors are back-propagated through the network. In WG, using the errors of each layer, gradients of the weights are calculated ($\frac{\partial error}{\partial w_i}$).

There are two parts to FPDeep: mapping and implementation (Fig.4). The Mapping Framework partitions a CNN into a number of fine-grained segments and maps them to FPGA clusters so that every FPGA gets a balanced workload and weights. In the Implementation Framework, the RTL generator creates RTL implementations for each FPGA based on the parameterized mapping, while a cycle-accurate simulator gives measures of throughput, percent idle stages, and bandwidth demand.

The two parts each have their own set of input parameters (see Table 1 and Fig.5). The network configuration parameters include 1) numbers (IC, OC) and sizes ($Ci * Ri, Co * Ro$) of the input and output feature maps, 2) convolution kernel size $KW * KH$, 3) stride size S , 4) padding size P_s , 5) activation function of each layer, 6) layer number, 7) layer type, 8) pooling function, and 9) pooling size P . Hardware constraints include 1) number of available FPGAs in the target cluster N , 2) on-chip memory resources per FPGA chip $BRAM$, 3) DSP resources per FPGA chip DSP , and 4) available transceiver channels per FPGA board $TRANS$.

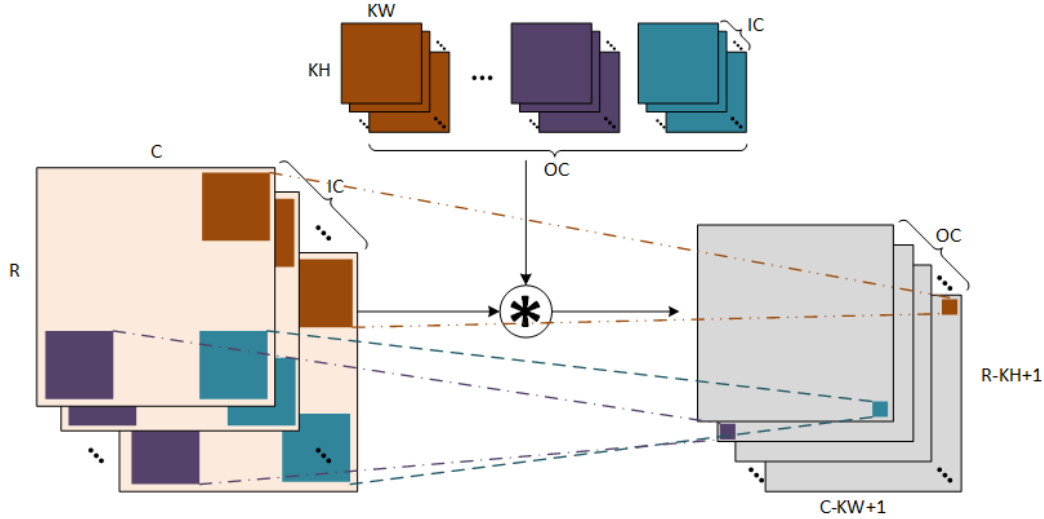


Figure 5: Illustration of CNN parameters defined in text

Algorithm 1: Pseudo Code of Convolution Layer

```

for  $R_o$  in Image.height do
  for  $C_o$  in Image.width do
    for  $f_o$  in out.channel.num do
      for  $f_i$  in in.channel.num do
        for  $k$  in Kernel.height do
          for  $l$  in Kernel.width do
             $out.fm[f_o][R_o][C_o] += weights[f_o + b][f_i][k][l] \times in.fm[f_i][R_o + k][C_o + l]$ 
          end
        end
      end
    end
  end
end

```

The organization of the rest of this and the next section is as follows. First, we describe how it is possible for FPDeep to implement a very deep, highly fine-grained pipeline, starting with a data dependency analysis of CNN training. Second, we present the mathematical model that is the basis for the mapping of CNN training to the distributed FPGA clusters. In the next section we describe the methods for partitioning and mapping and how they ensure balanced loads. We follow by describing how to allocate CNN weights among the FPGA devices so that each node's on-chip memory requirement is balanced and use of off-chip memory avoided.

3.2 Deep Fine-Grained Pipeline

The pseudo code of the convolution layer is shown in Algorithm 1. At each layer, IC feature maps are convolved by OC sets of $IC \times KW \times KH$ convolution kernels. For each kernel set, the convolution is performed by sliding the filters across feature maps. At each location, the resulting products of parameters and covered activations are summed, giving one activation at an output feature map. After OC iterations, every output feature map receives a new activation.

To illustrate data dependencies during training we use as an example two CONV layers with 3×3 kernel size. The operations of these two layers' forward/backward propagation are shown in Fig.6(A). In forward propagation, a 7×7 feature map is fed into Layer 1 and a 5×5 feature map is generated. At layer 2 the 5×5 feature map is convolved with the parameters and inferred to a 3×3 feature map. In the backward propagation, the 3×3 error map is padded to 7×7 before it is fed to Layer 2. Next, the error map and corresponding parameters are convolved and another (5×5) error map is produced; this is used for Layer 2's weight/bias gradient calculation. At Layer 1, the 5×5 error map is padded to 9×9 and then convolved to 7×7 .

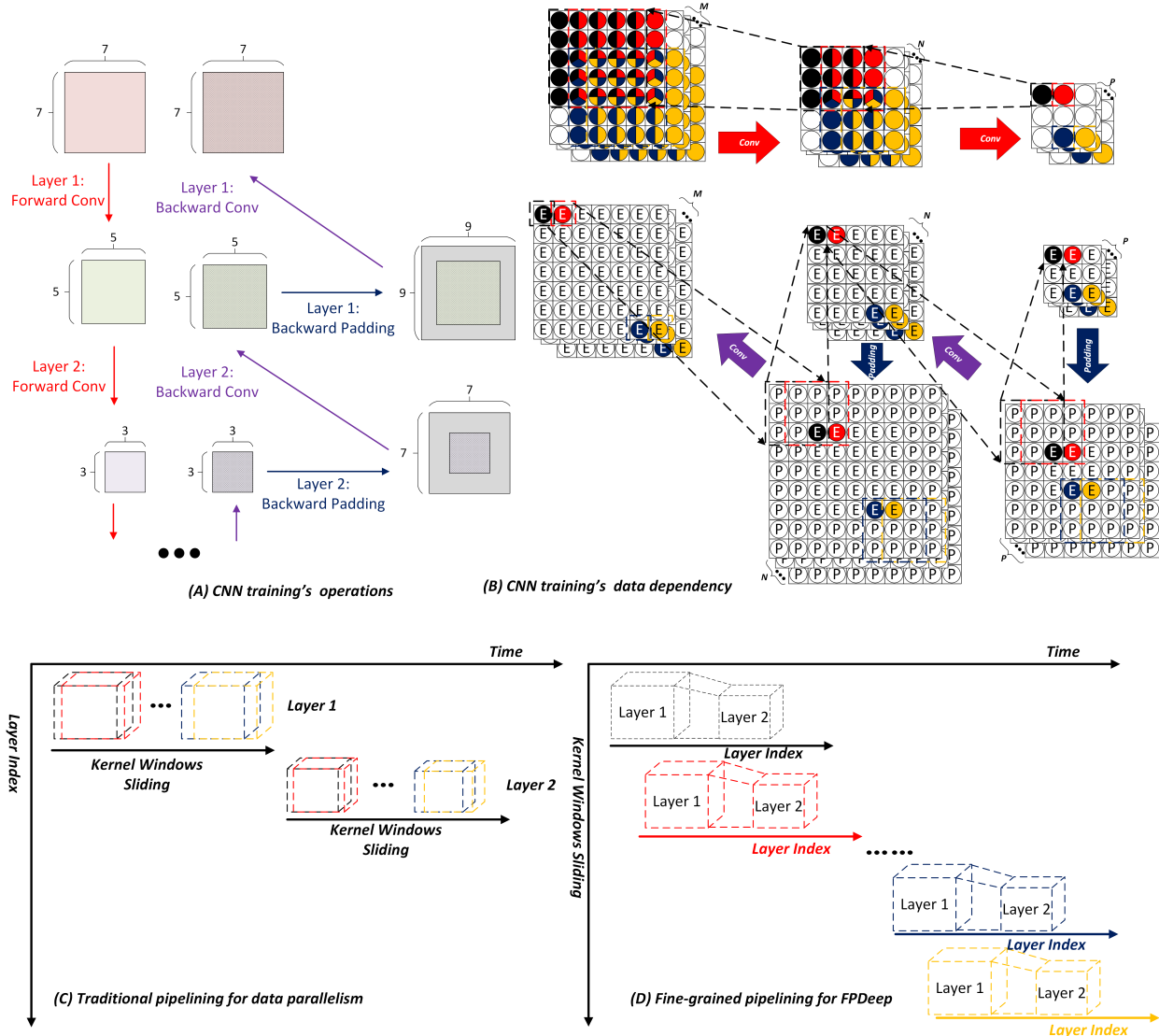


Figure 6: Network parameter

The Fig.6(B) depicts the data dependency of forwarding and backward propagations during CNN training. For the forward propagation phase, the image is inferred through all layers. To determine the data dependency, we start from the four activations at the output feature map at the last layer, which are marked as black, red, blue and yellow, respectively, and trace backwards to find the region of the input feature maps on which each depends. For the backward propagation phase, errors calculated are propagated backward through the network. To calculate gradients at a particular layer, errors which are backward propagated from the next layer and activations of its feature maps are necessary. Hence, the feature maps, which are generated in the forward propagation phase, need to remain available awaiting backward propagation. As shown in Fig.6, activations and errors among CONV layers show only fine-grained dependencies. That is, to begin computing the value of a pixel in a layer, only a fraction of the pixels from the previous layer are needed. Therefore the computation of a layer can start much earlier, before the previous layer is completely done. This provides the opportunity to process all CONV layers in parallel in a fine-grained pipeline.

The Fig.6(C) shows the traditional method of accelerating CNN training. First, the N channels of the feature maps are fed into convolution layer $L1$. Next, results from all M channels begin to be processed while the convolution kernel slides across the N -channel feature maps. Much storage capacity is needed to maintain all temporal feature maps. Clearly, this method is not efficient. The fine-grained alternative is shown in Fig.6(D): the calculation of an activation/error starts as soon as its dependent activations/errors are propagated from the previous/next layer. The basic

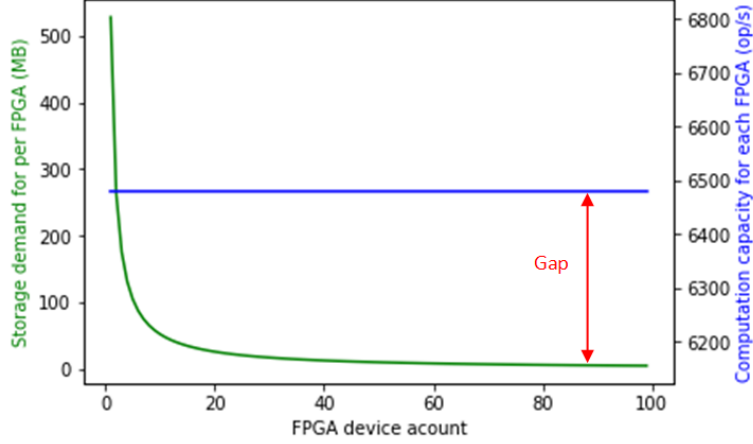


Figure 7: Compute capacity vs storage demand

process unit of FPDeep is an activation/error of a feature/error map; this is in contrast to the traditional method's basic unit of the entire feature/error map. The result is both a large increase in parallelism through the added pipeline stages and a reduction in storage so that only on-chip memory is needed.

3.3 Mathematical Model

We present a mathematical model based on the fine-grained pipelined mapping of CNN training to distributed FPGA clusters. Resource allocation is an optimization problem. The pipeline is constructed from Computation Engines (CEs), which are used to handle compute-intensive convolution operation, and buffers (Buf) to store CNN model weights and temporal feature maps. Convolution engines are composed of 2-D systolic array that consume the input features from shift-registers. Their design is similar to the ones in [14, 32]. The FPGAs' resources can be expressed as a tuple: $(LUT, FF, BRAM, DSP)$. The target function is to maximize the cluster's throughput (T). The constraints lie in the limited hardware resources at each device, which are denoted as $(LUT_{max}, FF_{max}, BRAM_{max}, DSP_{max})$.

The number of CEs is denoted as N_{CE} . The overall throughput (T) and number of buffers (N_{Buf}) are both functions of N_{CE} . We build part of CEs (αN_{CE}) with hard DSP slices and other CEs $((1 - \alpha)N_{CE})$ with LUTs/FFs. Similarly, some buffers (βN_{Buf}) are build with hard BRAMs and others $((1 - \beta)N_{Buf})$ with LUTs/FFs. Equation [1-6] defines the problem.

Target: Maximum throughput T

$$T = f_1(N_{CE}) \quad (1)$$

$$N_{Buf} = f_2(N_{CE}) \quad (2)$$

Subject to:

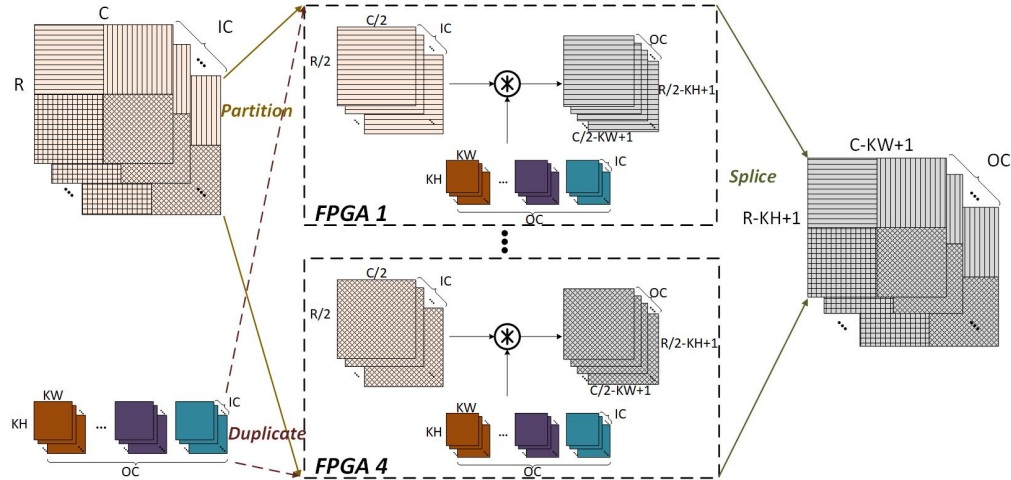
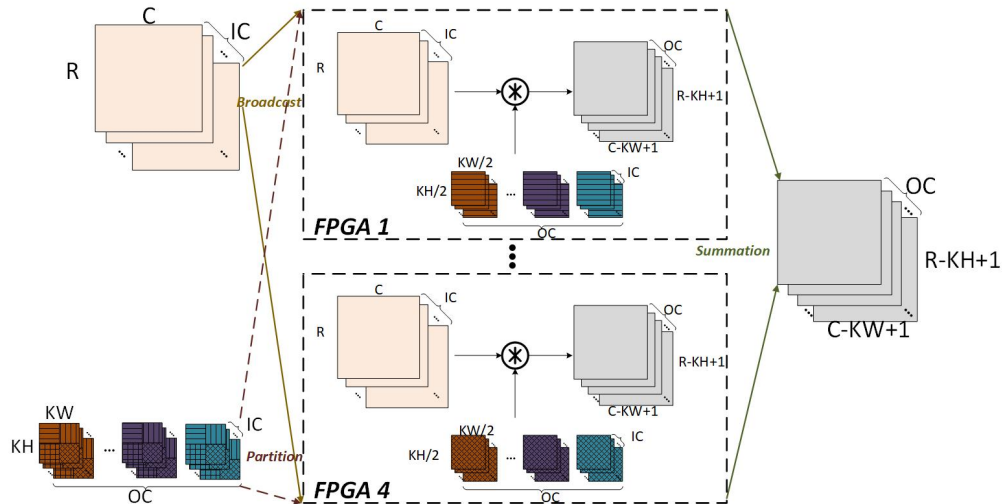
$$LUT = f_3(\alpha N_{CE}, \beta N_{Buf}, (1 - \alpha)N_{CE}, (1 - \beta)N_{Buf}) \leq LUT_{max}, \quad (3)$$

$$FF = f_4(\alpha N_{CE}, \beta N_{Buf}, (1 - \alpha)N_{CE}, (1 - \beta)N_{Buf}) \leq FF_{max} \quad (4)$$

$$BRAM = f_5(\beta N_{Buf}) \leq BRAM_{max} \quad (5)$$

$$DSP = f_6(\alpha N_{CE}) \leq DSP_{max} \quad (6)$$

As Fig.7 shows, the computational capacity of the cluster increase linearly with the number of available devices. However, since FPDeep uses model parallelism, a single execution pipeline is distributed over all of the FPGAs. The implication on storage demand is shown in Fig. 7: storage demand per device decreases as the number of FPGAs increases. The gap between computational capacity and storage demand shows that computation is the bottleneck and therefore also the larger challenge for load balancing (except for very small clusters).

Figure 8: Partition by image's row/column (r/c)Figure 9: Partition convolution kernel width/ kernel height (kw/kh)

4 Partitioning and Mapping for Load Balancing

4.1 Possible Partitions

We present four possible choices for partitioning the CNN training logic. Algorithm 1 and Fig.5 show the dimensions of the computation workload: image rows (r), image columns (c), image input channels (ic), image output channels (oc), kernel width (kw), and kernel height (kh). The possible partitions are by: 1) image's r/c ; 2) convolution kernel kw/kh ; or 3) by image channel ic/oc .

1) Partition by image's row/column (r/c). As shown in Fig.8, the input feature maps are partitioned into r/c dimension and each device handles part of image's convolution operations. A drawback of this method is that the CNN model weights need to be duplicated for each device. Also, during CNN training's back-propagation phase, the weight gradient descent results must be synchronized among all CNN model copies. This increases latency, which, in turn, increases the required memory since more activations must be stored. Furthermore, the activations and errors at the edges of these segments need to be shared by the neighbors, which makes the inter-device communication more complex.

2) Partition by convolution kernel width/ kernel height (kw/kh). As shown in Fig.9, all input feature maps are broadcast to the FPGAs and the CNN weights are partitioned into four pieces. Each device generates partial results of the

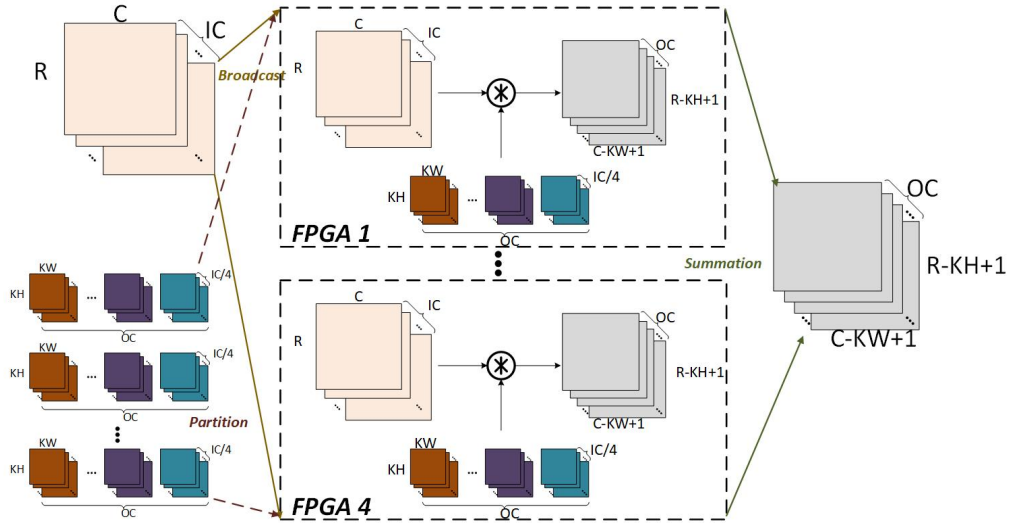


Figure 10: Partition image input channel ic

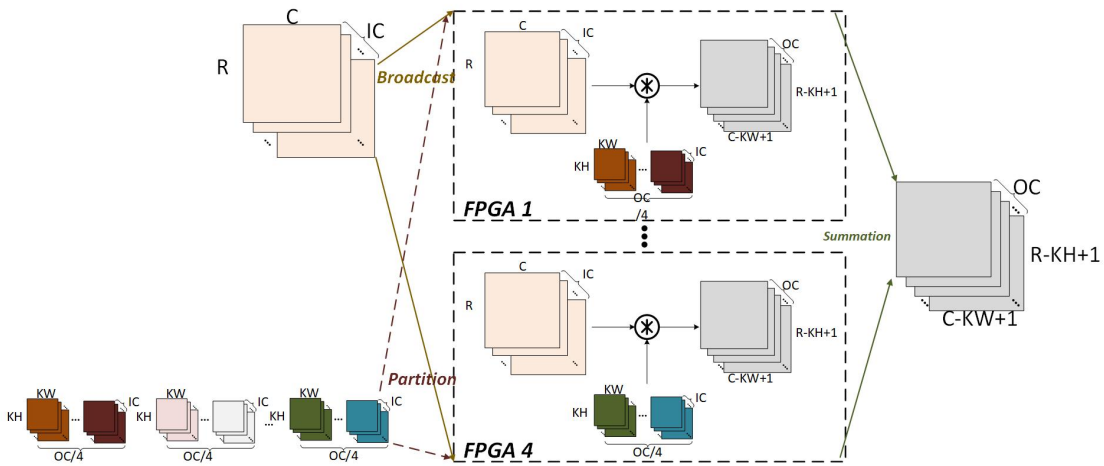


Figure 11: Partition image output channel oc

convolution layer and their sum is the final convolution result. In this method, only one copy of the CNN model weights is distributed. However, for most CNN networks, the size of convolution kernel is small (typically 3×3 or 5×5) so this partition does not provide enough parallelism for large clusters.

3) Partition by image input/output channel (ic/oc). As shown in Fig.10 and 11, each device executes the operations of a part of the input/output channels. Input feature maps, along with model parameters, are partitioned in the ic/oc dimension and allocated among FPGA devices. Each device generates the partial results and their sum is the final output features. In this method, only one copy of the CNN model is stored. For most of CNN networks, there are hundreds of activation channels resulting in sufficient parallelism. In short, partitioning by the images' input/output channels is our choice. In the following subsections, more details of the ic/oc partition method are presented.

4.2 Dataflow Analysis for CNN training

As shown in Fig.12(A), an N layer CNN is mapped to an FPGA cluster with M devices. Each CNN layer contains O_i operations ($i \in [1, N]$). The computation capacity of each device is C operation per second. To allocate balanced computation workloads among devices, and to minimize the idle stages of the whole fine-grained pipeline, the

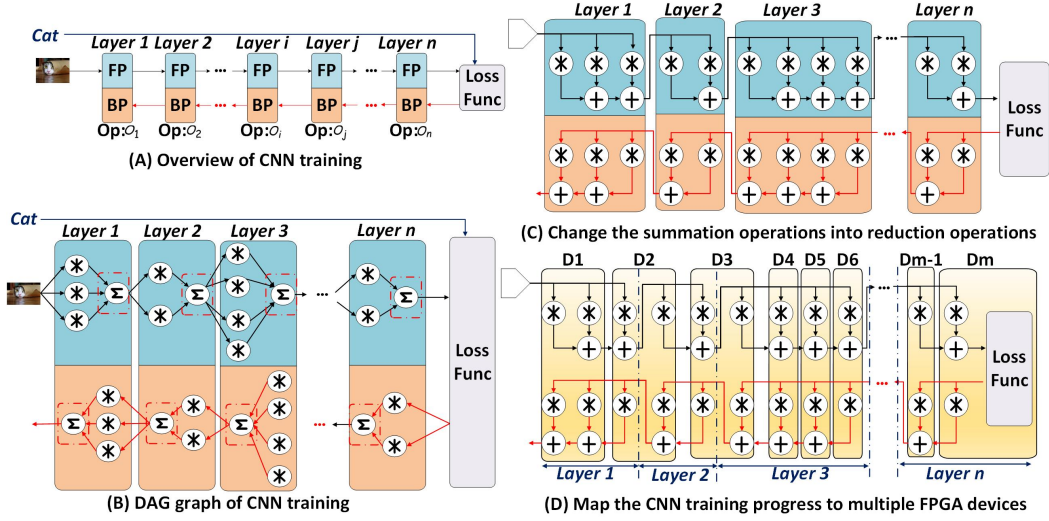


Figure 12: Data flow analyze of CNN training

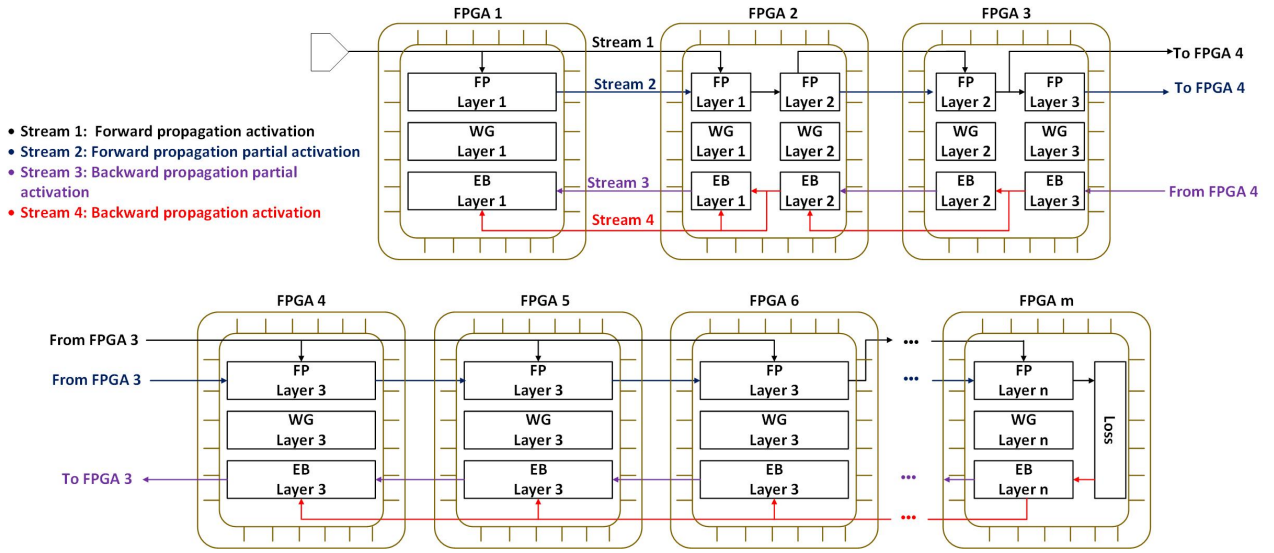


Figure 13: The data stream communication of the cluster and topology choice

computation workloads are mapped to different FPGA devices proportional to each device’s computation capacity. In other words, each device needs to execute $\bar{W} = \frac{\sum C_i}{M}$ operations.

Fig.12(B) zooms in on the CNN training procedure and turns the data flow graph into a directed acyclic graph (DAG). Sum operations highlighted by the red dotted boxes limit the scalability. Therefore, we transform the sum operations into several distributed reductions; the new DAG is shown in Fig.12(C). Continuing with Fig.12(C), the summation of all activation channels is cut into several pieces. Each piece only needs to add the local convolution result R_i to the previous node’s intermediate result R_{i-1} . In Fig.12(D), the workloads, i.e., the arithmetic operations, of a whole network are partitioned and mapped to M FPGA nodes proportionally to their computation capacities (the number of DSP slices and LUTs which can be used for computation). Fig.13 shows the data streams in the FPGA cluster (forward propagation activations, forward propagation partial activations, backward propagation activations, and backward propagation partial activations). Note that a 1-D interconnect topology is sufficient.

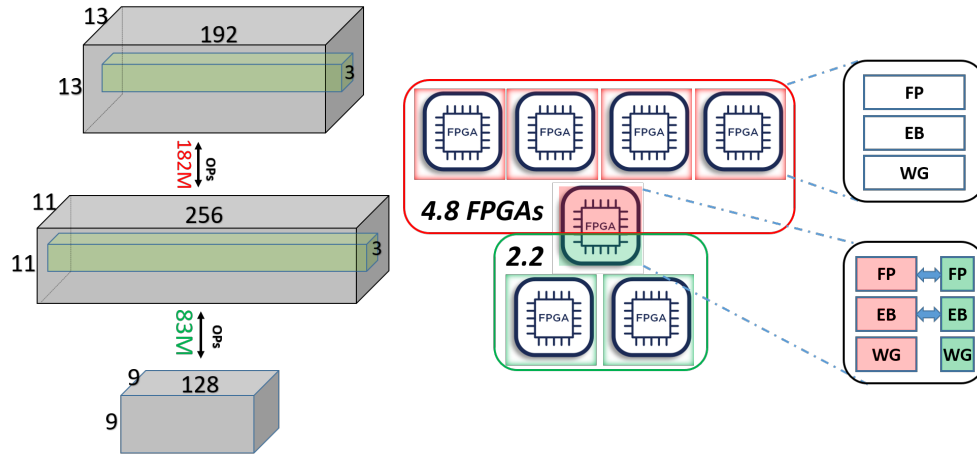


Figure 14: A 2-layer CNN to illustrate Inter-layer mapping. The 5th FPGA works for both layers. There are 2 sets of modules implemented in it: 1) FP, EB and WG modules for Layer1; 2) FP, EB and WG modules for layer 2.

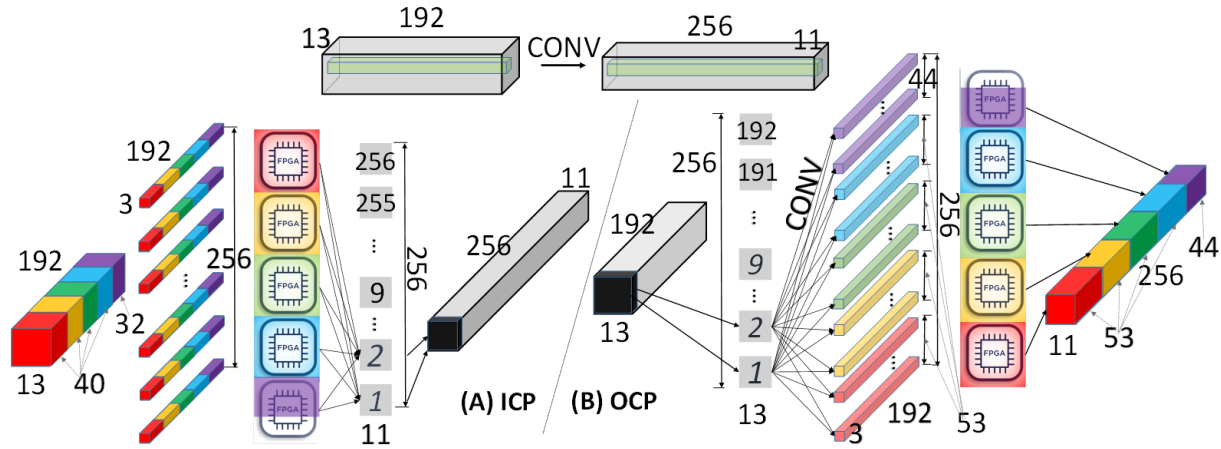


Figure 15: Illustration of ICP/OCP Overview

4.3 IC/OC partition implementation

We continue with more detail on how to implement the partition method with a 1-D topology; the dotted box in Fig.14 is used as an example. Layers 1 and 2 are mapped to seven FPGAs. FPGAs A D handle Layer 1 and FPGAs F G handle Layer 2. FPGA E works for both layers at the same time; with 80% used for Layer 1 and 20% for Layer 2. Partitioning by input and partitioning by output lead to very different results and their selection for each layer is an important part of FPDeep.

1) ICP: The ICP method is illustrated in Fig.15(A). Layer 1 is partitioned and mapped to 4.8 devices. 192 input features and corresponding weights are partitioned into 5 segments including 4 segments each containing 40 features and 1 smaller segment containing 32 features. Each FPGA receives one of the five segments and calculates partial results of features for all output channels. Each complete output feature is calculated by summing up the related partial results from the 5 FPGAs.

2) OCP: The OCP method is shown in Fig.15(B). 256 output features are partitioned into 5 segments, including 4 segments containing 53 output features and 1 smaller segment containing 44 features. Each FPGA is responsible for calculating a certain segment of output features. After joining all of the 5 segments results, the output feature channels of Layer 1 are complete. In CNN training, all activations need to remain available while waiting for back-propagation. Therefore, all 192 input feature maps are cached in every FPGA. This duplication leads to additional on-chip memory overhead. This defect of OCP does not exist in ICP, so FPDeep prefers to use ICP: OCP is only used when the number

of the input channel is too small to provide enough parallelism. For example, the first layer of AlexNet only has 3 channels of input features and 96 channels of output feature so OCP is used.

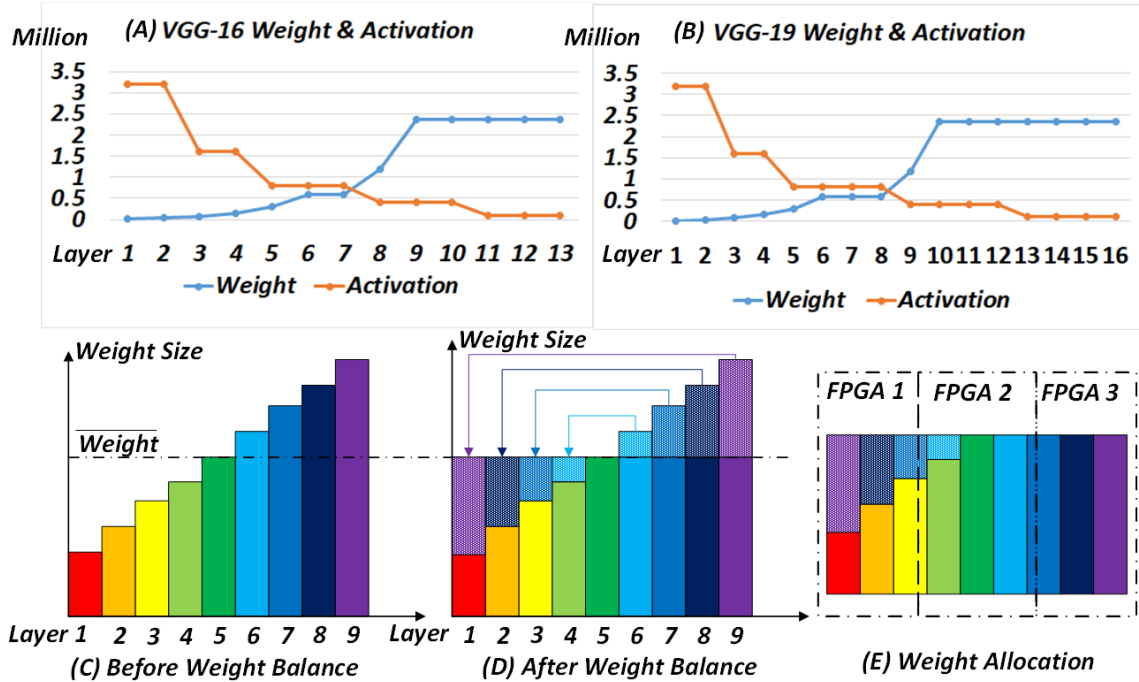


Figure 16: Weights and activations for VGG-16/19

4.4 Partitioning and Mapping the Weights

Figs.16(A&B) show the number of weights and activations of two VGGNets. Observe that from the first to the last layer, the number of activations is decreasing while the number of weights is increasing. The decrease of activations is because the dimensions of the feature maps are reduced by the pooling layers. The increase of the weights is because the number input and output channels increases in the later layers.

Using clusters with a small number of FPGAs to accelerate VGG-16 and VGG-19, the memory demands of weights for the FPGAs allocated to the later layers increase to the point where the on-chip memories in each FPGA are not big enough to cache the allocated weights. To make it possible to map big networks to a small number of FPGAs, weight balancing can be used. Figs.16(C-E) show the weight balancing methodology. Simply, weights from the later layers are stored in FPGAs where there is room, even if those FPGAs are some distance away from where those weights will eventually be used. For example, the weights of layer 8 are stored in FPGAs 3 and 1. During computation, the weights stored in FPGA 1 are transferred to the destination FPGA 3 through the 1D network together with activations. Note that the transport of weights does not tighten the constraint of inter-FPGA communication. This is because the smaller number of activations in the later layers cancels out the added traffic for the weights. Our experiments demonstrate the benefit of this approach: only on-chip memory is needed for the CONV layers.

5 Accelerator Implementation

We briefly sketch the accelerator implementation. FPDeep will be open-source and explained in detail in accompanying documentation.

As shown in Fig.17, each FPGA instance includes FP, WG, and EB modules, as well as a memory subsystem to cache weights, gradients, and activations. Each accelerator has 6 interconnection modules to communicate with its neighbors (this number is selected because it is available on many boards used for FPGA clusters and is sufficient for good scaling). An FPGA can be allocated to multiple layers. Implementations with FPGAs working for single layer and for multiple layers are illustrated in Fig.17(A) and (C).

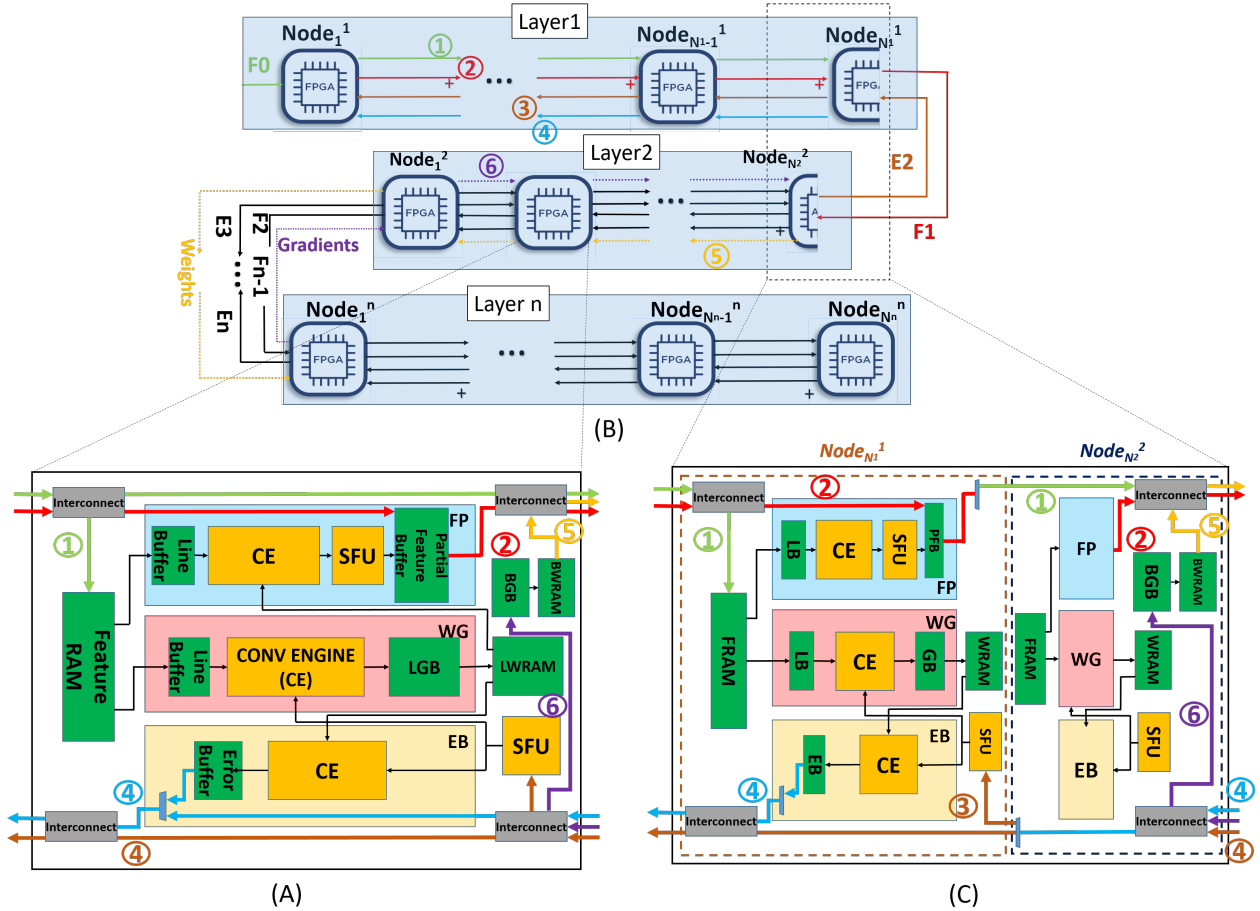


Figure 17: Overall architecture of FPDeep accelerator and block design of each FPGA. (A) illustrates the architecture of FPGA of $Node_2^2$ which is fully allocated to layer 2. (C) illustrates the architecture of FPGA of $Node_{N1}^1$ which is allocated to both layer1 and layer2. (B) illustrates the overall architecture of FPDeep; FPGAs can cooperatively work on the same layer and multiple layers can be mapped on the same FPGA. There are 6 key data-paths. Data-paths 1, 2 and 5 are for FP, while 3, 4 and 6 are for BP. Data-paths 1-4 have been discussed in Section 4.2. Data-path 5: Weights are transferred from the node where they are cached for weight load balancing to the node where they are used to compute the output features. Data-path 6: The gradients of weights are transferred from the node where they are produced to the node where they are cached for weight load balancing.

5.1 Memory Subsystem

The memory subsystem includes BRAM-based modules storing feature, weights and gradients.

1. Feature RAM (FRAM) caches input features mapped to the target FPGA until they are consumed in back-propagation and provides input features as operators to FP and WG modules.
2. Local Gradient Buffer (LGB) caches the gradients of the weights stored in LWRAM.
3. Balanced Gradient Buffer (BGB) caches the gradients of the weights stored BWRAM. These gradients are generated by and transferred from the node where the corresponding weights are consumed.
4. Local Weight RAM (LWRAM) caches weights used as operators to produce the output features at the local FPGA.
5. Balanced Weight RAM (BWRAM) BWRAM caches the weights mapped to the local device for weight load balancing. These weights are used as operators in other nodes where on-chip memory is not enough to cache all the required weights. Both LWRAM and BWRAM are updated by WG.

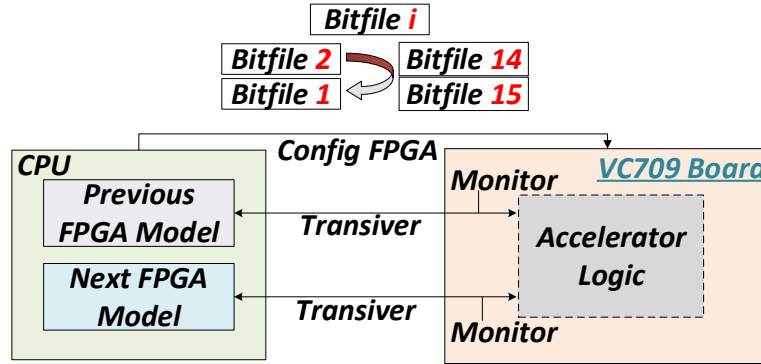


Figure 18: Evaluation experimental setup

5.2 Forward Propagation (FP)

The Line Buffer (LB) reads input features from the FRAM and feeds them to the Convolution Engines (CE) which are implemented as 2-D systolic arrays. The CEs perform convolutions with weights from the WRAM and input features from LB. In the Special Function Unit (SFU), the output features are activated, normalized, and sampled.

5.3 Error Back-Propagation (EB)

The EB module consumes errors of the next layer propagated by succeeding nodes and produces errors of the target layer. To calculate an error of a certain input feature map, errors of all output feature maps need to be convolved with respect to all weight filters. Errors of these input features are cached in the LB and propagated to the preceding node.

5.4 Weight Gradient Calculation (WG)

WG consumes errors of the next layer propagated from the succeeding neighbor and calculates gradients of weights and biases. To obtain gradients of weights, errors of output feature maps are used as a filter and convolved with input feature maps cached in the FRAM. Gradients are cached in the Gradient Buffer and used to update weights in WRAM.

6 Experimental Results

In this section, we describe experiments performed to evaluate the efficiency of FPDeep. First, we evaluate the design of each FPGA generated by FPDeep based on real implementations. Second, we evaluate the performance of the cluster-level design of FPDeep based on results of the FPDeep simulator.

6.1 Single FPGA Implementation and Experiments

Results in this subsection are generated with a single FPGA board. We use FPDeep to map three of the most widely used CNNs—Alexnet, VGGNet-16 and VGGNet-19—onto a 15-FPGA cluster. For each network, the RTL generator creates 15 bitfiles, one for each FPGA. The experimental setup is shown in Fig.18.

We evaluate the design of each FPGA separately with a Xilinx VC709 board (Virtex7 XC7VX690T) and gather resource utilization, throughput, and bandwidth requirements. Stochastic rounding is used during low-precision fixed-point training. In [33], it is proven that CNNs can be trained using only 16-bit fixed-point numbers when using stochastic rounding and incur no degradation in classification accuracy.

Figs.19(A-L) shows resource utilizations of each FPGA and resource allocations among AlexNet, VGGNet-16 and VGGNet-19 layers. As shown in Figs.19(D)(H)(L)'s DSP utilization report, the mapping is well-balanced. The usage of DSP slices is roughly 80% and the throughput of each FPGA matches, around 1 TOPS. Only on-chip BRAM is used in the FPGAs that work solely on the CONV layers (FPGAs 1-14) and utilizations of BRAMs are under 80%. The highest bandwidth requirement among these 15 FPGAs for these three networks is 18.6 Gb/s.



Figure 19: Experiment results and utilization report

Table 2 shows a performance and power efficiency comparison among Titan X GPU [6], Tesla K80 GPU [34], a previous FPGA [6] implementation, and our work. FPDeep provides performance which is $5\times$ higher than previous FPGA work and comparable to the Titan X GPU. We evaluate energy efficiency with respect to GOPs/J. FPDeep provides $8.8\times$ better energy efficiency than Titan X and $5.6\times$ better than the previous FPGA work. Compared with the K80, FPDeep provides $5.7\times$ better energy efficiency.

6.2 Cluster-Level Performance Evaluation

We use a cycle-accurate simulator to evaluate cluster-level performance. Alexnet, VGG-16, and VGG-19 are mapped onto clusters of sizes 5 to 85. To demonstrate that the workload among FPGAs remains balanced in different sized clusters, we present the proportions of idle stages. Figs.20(B)(E)(H) shows that the proportion of idle stages is always under 5%. When the number of FPGAs is more than 30, the number of idle stages is stable with fluctuation of only from 0.5% to 1%. Generally, as the number of FPGAs increases, the proportion of idle stages decreases. The reason is that during IFP and OFP, the number of DSPs allocated to each layer is rounded to a multiple of $K \times K$. With more FPGAs and more DSP resources, the effects of rounding error are lessened.

Table 2: CLUSTER-LEVEL EXPERIMENTAL RESULT

	CPU [6]	GPU [6]	GPU		FPGA[6]		Our Work		
Device	AMD A10	Titan X	Tesla K80		XC7VX690T				
CNN Model	AlexNet	AlexNet	AlexNet [34]	VGG-16 [35]	AlexNet	VGG-16	AlexNet	VGG-16	VGG-19
Config	1 CPU	1 GPU	1 GPU	1 GPU	4 FPGA	1 FPGA	15 FPGA	15 FPGA	15 FPGA
Precision	floating	floating	floating	floating	fixed 16				
Perf (GOPS)	34.23	1385	2330	2018	207 (Per FPGA)	290 (Per FPGA)	1157(Per FPGA)	1197(Per FPGA)	1220(Per FPGA)
Training time (H) Per Epoch	-	-	-	-	-	-	0.17	2.19	2.76
Power efficiency (GOPS/J)	0.39	4.22	7.87	6.86	6.55	8.28	37.09	37.88	38.13

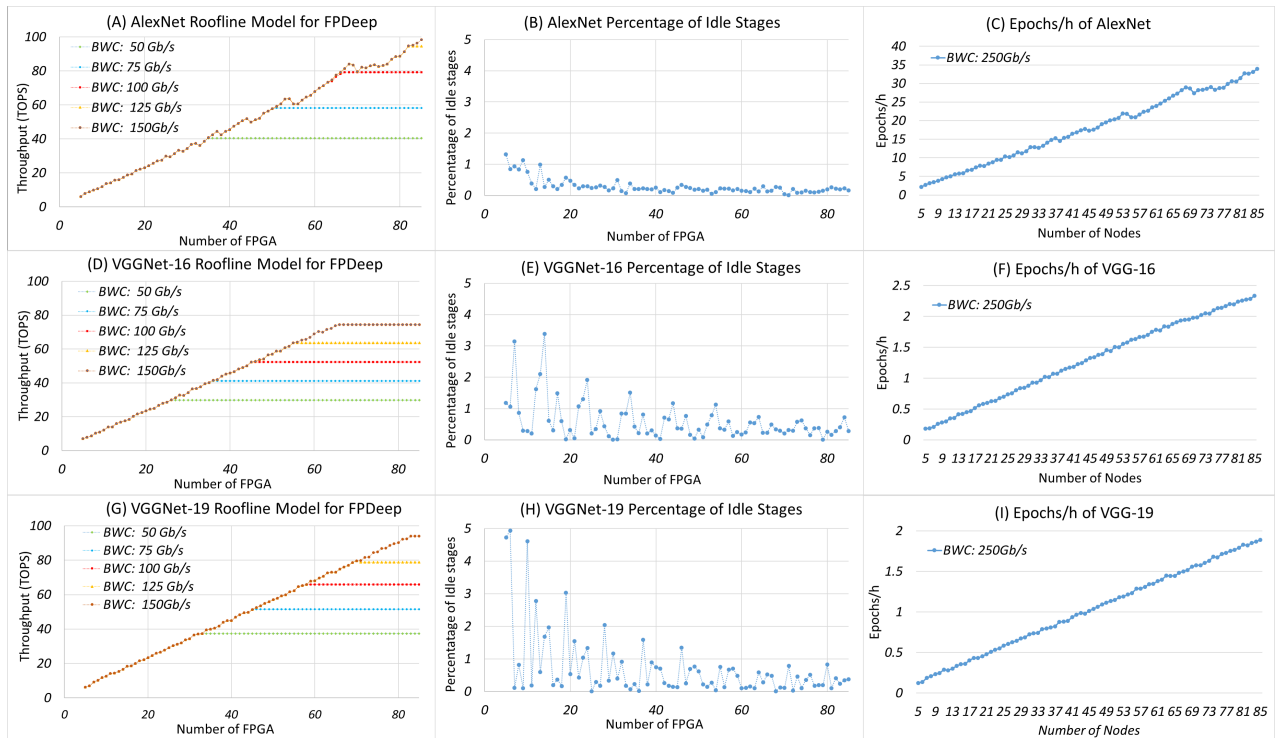


Figure 20: Roofline Models, Percentages of Idle stages and Epochs per hour of AlexNet, VGGNet-16 and VGGNet-19

Computation and communication are the two most critical constraints in system throughput optimization. The roofline plots of AlexNet, VGG-16, and VGG-19 are shown in Figs.20(A)(D)(G). The whole system throughput presents excellent linear scalability, up to a constraint imposed by the inter-FPGA communication bottleneck. For example, with 150 Gbps as the inter-board communication constraint, FPDeep shows linearity up to 83, 56, 70 FPGAs among Alexnet, VGG-16 and VGG-19 respectively. As each transceiver (of that generation) can reach a maximum rate of 28 Gb/s, using 6 transceivers per FPGA achieves this number [36, 37, 38].

Since high-end FPGAs frequently have more than 50 transceivers, scaling to much larger clusters is possible. The reason that bandwidth required by VGG-16 is larger than VGG-19 is straightforward: VGG-19 has more layers and thus more workload. During partitioning, with the same overall hardware resources, each layer of VGG-19 is allocated

fewer resources. Thus, fewer batch (B_f, B_w, B_e) features in each layer can be computed and transferred in parallel, which results in a smaller bandwidth requirement.

Comparing AlexNet with VGGNets, we observe that AlexNet requires less bandwidth than both VGGNets, despite having a lower workload. Using an 85-FPGA cluster as an example, the communication bottleneck of all three networks is located at the 2nd layer. For Alexnet, K and F_i of layer 2 are bigger than that of the VGGNets, which means that computing each output feature requires more resources. Although the 2nd layer of AlexNet is allocated with more resources, B of Alexnet is still smaller than that of the other two networks. B_e s of the 2nd layer are 12, 16, 13 for Alexnet, VGG-16, and VGG-19 respectively.

Figs.20(C)(F)(I) shows the number of epochs that can be trained per hour. FPDeep provides linear speedup of training per epoch. As hybrid model/layer parallelism does not constrain the choice of mini-batch size, the optimal learning rate and mini-batch size can always be applied in SGD, leading to the minimal number of epochs needed to be trained for a certain accuracy. Hence, linear speedup of training per epoch results in linear speedup of CNN training.

7 Conclusion

In this paper, we propose a framework, FPDeep, which maps training logic of CNNs to a multi-FPGA cluster efficiently with workload balancing, and also automatically generates RTL implementations for the target networks.

With FPDeep, clusters of FPGAs work in a deeply-pipelined manner using 1-D topology; this enables the accelerators to map directly onto existing platforms, including Catapult, Catapult2, and almost any tightly-coupled FPGA cluster. FPDeep uses two mechanisms to facilitate high-performance and energy-efficiency: 1) various fine-grained partition and mapping strategies to balance workload among FPGAs, and 2) training of CNNs is executed in a fine-grained inter- and intra-layer pipelined manner, which reduces the time features need for backward propagation, leading to reduced storage demand to the point where only on-chip memory is required for CONV layers. Experiments show that FPDeep has good scalability to a large number of FPGAs. The bottleneck is the inter-FPGA communication bandwidth. Using Alexnet and the VGGNets as benchmarks, with 6 transceivers per FPGA, FPDeep shows linearity up to 83 FPGAs. We evaluate energy efficiency with respect to GOPs/J and find that FPDeep provides 5.7x to 8.8x higher energy efficiency than GPU servers.

Currently, we are implementing FPDeep on the AWS FPGA cloud and will then make FPDeep open source.

8 Acknowledgement

This research was partially funded by the Deep Learning for Scientific Discovery Investment under Pacific Northwest National Laboratory's Laboratory Directed Research and Development Program. The Pacific Northwest National Laboratory is operated by Battelle for the U.S. Department of Energy under contract DE-AC05-76RL01830. This work was also supported, in part, by the NSF through Awards CNS-1405695 and CCF-1618303/7960; by the NIH through Award 1R41GM128533; by grants from Microsoft and Red Hat; and by Intel through donated FPGAs, tools, and IP.

Preliminary versions of parts of this work have been published in FCCM 2018 [39] and FPL 2018 [40].

References

- [1] Shuang Liang, Shouyi Yin, Leibo Liu, Wayne Luk, and Shaojun Wei. FP-BNN: binarized neural network on FPGA. *Neurocomputing 2018*, 275:1072–1086, 2018.
- [2] Xing Sun, Zhimin Xu, Nan Meng, Edmund Lam, and Hayden K-H So. Data-driven light field depth estimation using deep convolutional neural networks. In *IJCNN 2016*, pages 367–374, 2016.
- [3] Ruizhe Zhao, Xinyu Niu, Yajie Wu, Wayne Luk, and Qiang Liu. Optimizing cnn-based object detection algorithms on embedded FPGA platforms. In *ARC 2017*, pages 255–267, 2017.
- [4] Swagath Venkataramani, Ashish Ranjan, Subarno Banerjee, Dipankar Das, Sasikanth Avancha, Ashok Jagannathan, Ajaya Durg, Dheemanth Nagaraj, Bharat Kaul, Pradeep Dubey, et al. Scaleddeep: A scalable compute architecture for learning and evaluating deep networks. *sigarch comput. archit. news* 45, 2 (june 2017), 13–26, 2017.
- [5] Priya Goyal, Piotr Dollár, Ross Girshick, Pieter Noordhuis, Lukasz Wesolowski, Aapo Kyrola, Andrew Tulloch, Yangqing Jia, and Kaiming He. Accurate, large minibatch sgd: training imagenet in 1 hour. *arXiv preprint arXiv:1706.02677*, 2017.

- [6] Chen Zhang, Di Wu, Jiayu Sun, Guangyu Sun, Guojie Luo, and Jason Cong. Energy-efficient cnn implementation on a deeply pipelined fpga cluster. In *ISLPED 2016*, pages 326–331. ACM, 2016.
- [7] Ahmed Sanaullah, Chen Yang, Yuri Alexeev, Kazutomo Yoshii, and Martin C Herbordt. Application aware tuning of reconfigurable multi-layer perceptron architectures. In *2018 IEEE High Performance extreme Computing Conference (HPEC)*, pages 1–9. IEEE, 2018.
- [8] Ahmed Sanaullah, Chen Yang, Yuri Alexeev, Kazutomo Yoshii, and Martin C Herbordt. Trip: An ultra-low latency, teraflops/s reconfigurable inference processor for real-time multi-layer perceptrons. *2017 The International Conference for High Performance Computing, Networking, Storage and Analysis (Supercomputing)*, 2017.
- [9] Ahmed Sanaullah, Chen Yang, Yuri Alexeev, Kazutomo Yoshii, and Martin C Herbordt. Real-time data analysis for medical diagnosis using fpga-accelerated neural networks. *BMC bioinformatics*, 19(18):490, 2018.
- [10] Chen Zhang, Peng Li, Guangyu Sun, Yijin Guan, Bingjun Xiao, and Jason Cong. Optimizing fpga-based accelerator design for deep convolutional neural networks. In *Proceedings of the 2015 ACM/SIGDA International Symposium on Field-Programmable Gate Arrays*, pages 161–170. ACM, 2015.
- [11] Liqiang Lu, Yun Liang, Qingcheng Xiao, and Shengen Yan. Evaluating fast algorithms for convolutional neural networks on fpgas. In *Field-Programmable Custom Computing Machines (FCCM), 2017 IEEE 25th Annual International Symposium on*, pages 101–108. IEEE, 2017.
- [12] Eric Chung, Jeremy Fowers, Kalin Ovtcharov, Michael Papamichael, Adrian Caulfield, Todd Massengill, Ming Liu, Daniel Lo, Shlomi Alkalay, Michael Haselman, et al. Serving dnns in real time at datacenter scale with project brainwave. *IEEE Micro*, 38(2):8–20, 2018.
- [13] Jeremy Fowers, Kalin Ovtcharov, Michael Papamichael, Todd Massengill, Ming Liu, Daniel Lo, Shlomi Alkalay, Michael Haselman, Logan Adams, Mahdi Ghandi, et al. A configurable cloud-scale dnn processor for real-time ai. In *Proceedings of the 45th Annual International Symposium on Computer Architecture*, pages 1–14. IEEE Press, 2018.
- [14] Wenlai Zhao, Haohuan Fu, Wayne Luk, Teng Yu, Shaojun Wang, Bo Feng, Yuchun Ma, and Guangwen Yang. F-cnn: An fpga-based framework for training convolutional neural networks. In *ASAP 2016*, pages 107–114, 2016.
- [15] Yijin Guan, Hao Liang, Ningyi Xu, Wenqiang Wang, Shaoshuai Shi, Xi Chen, Guangyu Sun, Wei Zhang, and Jason Cong. Fp-dnn: An automated framework for mapping deep neural networks onto fpgas with rtl-hls hybrid templates. In *FCCM 2017*, pages 152–159, 2017.
- [16] Jason Cong, Vivek Sarkar, Glenn Reinman, and Alex Bui. Customizable domain-specific computing. *IEEE Design & Test of Computers 2011*, 28:6–15, 2011.
- [17] Gopalakrishna Hegde, Nachiket Kapre, et al. CaffePresso: Accelerating Convolutional Networks on Embedded SoCs. *TECS 2018*, 17(1):15, 2018.
- [18] Duncan JM Moss, Eriko Nurvitadhi, Jaewoong Sim, Asit Mishra, Debbie Marr, Suchit Subhaschandra, and Philip HW Leong. High performance binary neural networks on the Xeon+ FPGA platform. In *FPL 2017*, pages 1–4, 2017.
- [19] Ruo Long Lian. *A framework for FPGA-based acceleration of neural network inference with limited numerical precision via high-level synthesis with streaming functionality*. PhD thesis, University of Toronto, 2016.
- [20] Tal Ben-Nun and Torsten Hoefler. Demystifying parallel and distributed deep learning: An in-depth concurrency analysis. *arXiv preprint arXiv:1802.09941*, 2018.
- [21] Michaela Blott, Thomas B Preußer, Nicholas Fraser, Giulio Gambardella, Kenneth O’Brien, Yaman Umuroglu, and Miriam Leeser. Scaling neural network performance through customized hardware architectures on reconfigurable logic. In *ICCD 2017*, pages 419–422, 2017.
- [22] Tianqi Chen, Mu Li, Yutian Li, Min Lin, Naiyan Wang, Minjie Wang, Tianjun Xiao, Bing Xu, Chiyuan Zhang, and Zheng Zhang. Mxnet: A flexible and efficient machine learning library for heterogeneous distributed systems. *arXiv preprint arXiv:1512.01274*, 2015.

- [23] Yangqing Jia, Evan Shelhamer, Jeff Donahue, Sergey Karayev, Jonathan Long, Ross Girshick, Sergio Guadarrama, and Trevor Darrell. Caffe: Convolutional architecture for fast feature embedding. In *Proceedings of the 22nd ACM international conference on Multimedia 2014*, pages 675–678. ACM, 2014.
- [24] Martín Abadi, Ashish Agarwal, Paul Barham, Eugene Brevdo, Zhifeng Chen, Craig Citro, Greg S Corrado, Andy Davis, Jeffrey Dean, Matthieu Devin, et al. Tensorflow: Large-scale machine learning on heterogeneous distributed systems. *arXiv preprint arXiv:1603.04467*, 2016.
- [25] Kalin Ovtcharov, Olatunji Ruwase, Joo-Young Kim, Jeremy Fowers, Karin Strauss, and Eric S Chung. Accelerating deep convolutional neural networks using specialized hardware. *Microsoft Research Whitepaper 2015*, 2(11), 2015.
- [26] Adrian M Caulfield, Eric S Chung, Andrew Putnam, Hari Angepat, Jeremy Fowers, Michael Haselman, Stephen Heil, Matt Humphrey, Puneet Kaur, Joo-Young Kim, et al. A cloud-scale acceleration architecture. In *MICRO 2016*, pages 1–13, 2016.
- [27] Mu Li, David G Andersen, Jun Woo Park, Alexander J Smola, Amr Ahmed, Vanja Josifovski, James Long, Eugene J Shekita, and Bor-Yiing Su. Scaling distributed machine learning with the parameter server. In *OSDI*, volume 14, pages 583–598, 2014.
- [28] Xiangru Lian, Ce Zhang, Huan Zhang, Cho-Jui Hsieh, Wei Zhang, and Ji Liu. Can decentralized algorithms outperform centralized algorithms? a case study for decentralized parallel stochastic gradient descent. In *Advances in Neural Information Processing Systems*, pages 5330–5340, 2017.
- [29] Jianmin Chen, Xinghao Pan, Rajat Monga, Samy Bengio, and Rafal Jozefowicz. Revisiting distributed synchronous sgd. *arXiv preprint arXiv:1604.00981*, 2016.
- [30] Yonghui Wu, Mike Schuster, Zhifeng Chen, Quoc V Le, Mohammad Norouzi, Wolfgang Macherey, Maxim Krikun, Yuan Cao, Qin Gao, Klaus Macherey, et al. Google’s neural machine translation system: Bridging the gap between human and machine translation. *arXiv preprint arXiv:1609.08144*, 2016.
- [31] Alex Krizhevsky, Ilya Sutskever, and Geoffrey E Hinton. Imagenet classification with deep convolutional neural networks. In *Advances in neural information processing systems*, pages 1097–1105, 2012.
- [32] Xuechao Wei, Cody Hao Yu, Peng Zhang, Youxiang Chen, Yuxin Wang, Han Hu, Yun Liang, and Jason Cong. Automated systolic array architecture synthesis for high throughput cnn inference on fpgas. In *Proceedings of the 54th Annual Design Automation Conference 2017*, page 29. ACM, 2017.
- [33] Ankur Agrawal Kailash Gopalakrishnan Gupta, Suyog and Pritish Narayanan. Deep learning with limited numerical precision. In *ICML 2015*, pages 1737–1746, 2016.
- [34] LeaderGPU. Tensorflow Alexnet benchmark. <https://www.leadergpu.com/articles/428-tensorflow-alexnet-benchmark>, 2018. [Online; accessed 19-July-2018].
- [35] LeaderGPU. Tensorflow VGG-16 benchmark. <https://www.leadergpu.com/articles/430-tensorflow-vgg16-benchmark>, 2018. [Online; accessed 19-July-2018].
- [36] Jiayi Sheng, Chen Yang, Tianqi Wang, and Martin Herbordt. High performance dynamic communication on reconfigurable clusters. In *2018 IEEE 26th Annual International Symposium on Field-Programmable Custom Computing Machines (FCCM)*, pages 219–219. IEEE, 2018.
- [37] Jiayi Sheng, Chen Yang, and Martin C Herbordt. High performance communication on reconfigurable clusters. In *2018 28th International Conference on Field Programmable Logic and Applications (FPL)*, pages 219–2194. IEEE, 2018.
- [38] Alan D George, Martin C Herbordt, Herman Lam, Abhijeet G Lawande, Jiayi Sheng, and Chen Yang. Novo-g#: Large-scale reconfigurable computing with direct and programmable interconnects. In *High Performance Extreme Computing Conference (HPEC), 2016 IEEE*, pages 1–7. IEEE, 2016.
- [39] Tong Geng, Tianqi Wang, Ahmed Sanoullah, Chen Yang, Rui Xu, Rushi Patel, and Martin Herbordt. Fpdeep: Acceleration and load balancing of cnn training on fpga clusters. In *2018 IEEE 26th Annual International Symposium on Field-Programmable Custom Computing Machines (FCCM)*, pages 81–84. IEEE, 2018.
- [40] Tong Geng, Tianqi Wang, Ahmed Sanoullah, Chen Yang, Rushi Patel, and Martin Herbordt. A framework for acceleration of cnn training on deeply-pipelined fpga clusters with work and weight load balancing. In *2018 28th International Conference on Field Programmable Logic and Applications (FPL)*, pages 394–3944. IEEE, 2018.